Supplementary Information for

Optimizing electrochemical alcohols oxidation reactions via defect-rich CoFe-layered double hydroxide

Xingjian Sun, Ruikang Zhang,* Han Lu, Qichao Yan, Sicong Sun, Yuanzhe Gao*

Hebei Technology Innovation Center for Energy Conversion Materials and Devices, College of Chemistry and Materials Science, Hebei Normal University, Shijiazhuang, Hebei 050024, China

E-mail: zhangruikang@hebtu.edu.cn (R. Zhang)

E-mail: yzgao2003@126.com (Y. Gao)

Experimental Details

All potentials in this work were adjusted to the reversible hydrogen electrode (RHE), according to the equation: $E_{RHE} = E_{applied} + E_{Hg/HgO} + 0.0592pH$. The Tafel slope was calculated from the Tafel equation as follows: $\eta = b \log i$, where η is the overpotential and b is the Tafel slope.

CoFe-LDH and CoFe-LDH-Don the nickel foam were sonicated to collect the powder. Then, the powder was acidified with 0.1 M HCl and finally the metal ion concentration was tested by inductively coupled plasma atomic emission spectrometer (ICP-AES). The liquid product is detected by taking 1 ml of electrolyte and performing a nuclear magnetic test with dimethyl sulfoxide (DMSO, 99.9%) as a solvent.

The Faradaic efficiency (FE) of acetate was calculated as: $FE = (n \times c \times V \times F/Q)$

*100%, where n is the number of transferred electrons, for acetate, n = 4, F is the Faraday constant, c is the concentration of acetate in the electrolyte as determined by ion chromatography, V is the volume of the electrolyte used for ethanol oxidationelectrolyte, and Q is the quantity of applied electric charges during the chronoamperometric measurements of EOR. (In this experiment, we took 1 ml electrolyte and then diluted 50 times for ion chromatography to detect acetate concentration; Q is given by the automatic integration given by the electrochemical work station.)

The coverage (τ*) was calculated as:$Ip = (n^2F^2/4RT)\nu A\tau^*$. In this formula, Ip represents the Co redox peak current density, n is the number of electrons involved in the transfer (Co^{3+}/Co^{4+}, n= 1), F is the Faraday constant (96845 C mol^{-1}), R is the ideal gas constant (8.314 J^{-1} mol^{-1}), T is the temperature maintained at 298.15 K, ν is the scanning rate of the cyclic voltammetric curve, A refers to the geometric surface area of the glassy carbon electrode which is 0.196 cm^2, and τ* indicates the surface coverage of the redox-active species.

Computational Details:

CoFe-LDH and CoFe-LDH-D models: The models were built on the basis of XRD and ICP-AAS results. The space group is p3m1, with lattice parameter $\alpha = \beta =$ 90°, γ = 120°. The (003) and (110) facet of NiFe-LDH were located at 2θ= 11.41° and 59.94°, respectively. the lattice parameters deduced to be a = b = 3.08 Å, and c = 7.17 Å. The supercell of CoFe-LDH is set to be 5 × 3 × 1 in the a-, b-, and c-direction. CoFe-LDH model. Chloride anions are placed into the interlayer gallery of LDHs to

keep the charge neutral. The atomic numbers of Co-Fe-O-H-Cl were 11-4-30-30-4 in the CoFe-LDH. One Fe atom were removed from CoFe-LDH model to built CoFe-LDH-D model.

Computational Methods: All the calculations are performed using the Forcite code in the Materials Studio, version 6.1 software package. The geometry optimizations are based on the following points: (1) Forcefield is Universal; (2) the electrostatic is Ewald; (3) the quality is Ultra-fine. The adsorption models is created by installing the LDH slab on the (001) surface, and the vacuum distance here is set to be 30 Å to eliminate the interactions between the replicas of the slab model. Adsorption Locator tools are used to investigate the minimum adsorption energies of the intermediate species.

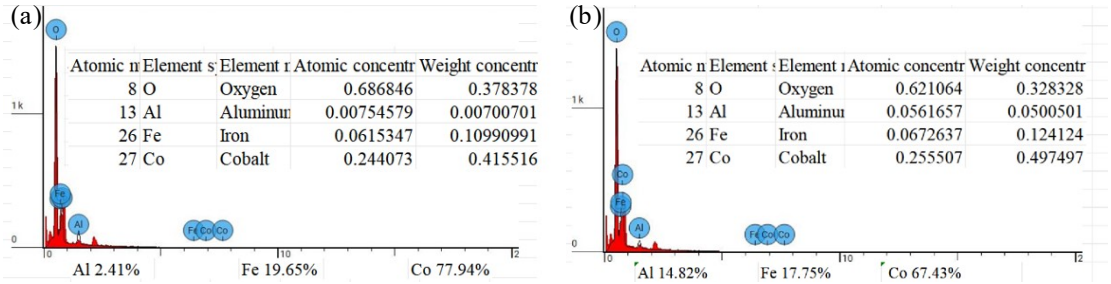

Fig. S1 The EDS of (a) CoFe-LDH-D and (b) CoFeAl-LDH.

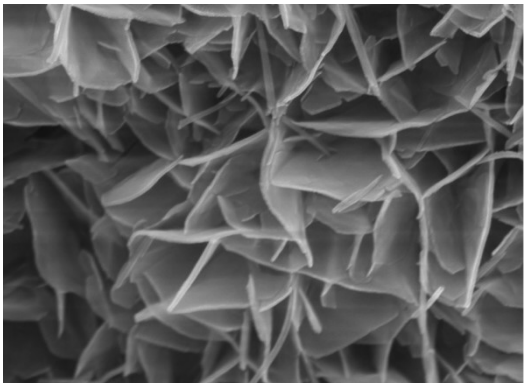

Fig. S2 SEM images of CoFe-LDH.

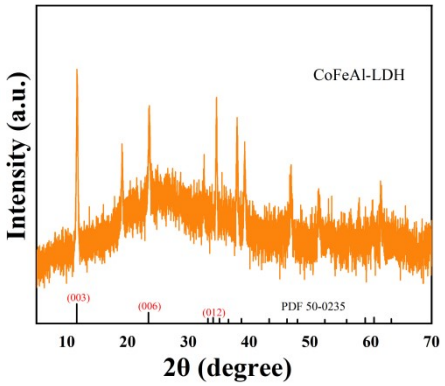

Fig. S3 XRD patterns of CoFeAl-LDH.

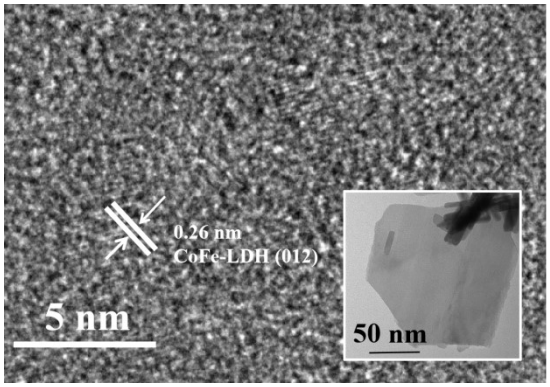

Fig. S4 The TEM imagine of CoFe-LDH.

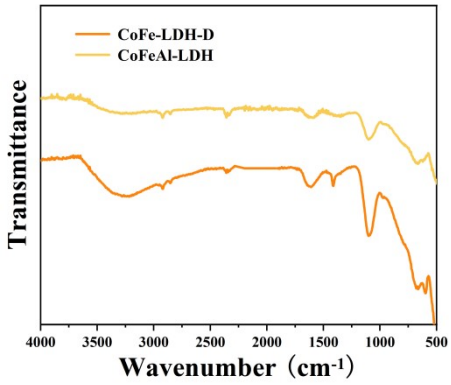

Fig. S5 The FT-IR spectroscopy of CoFe-LDH-D and CoFeAl-LDH.

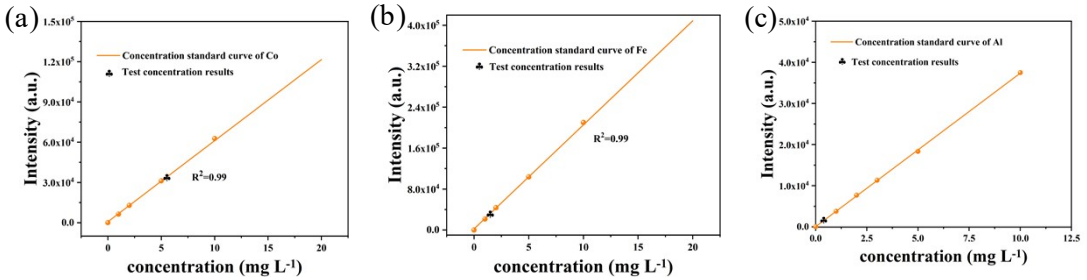

Fig. S6 The correction curve of the Co, Fe, Al.

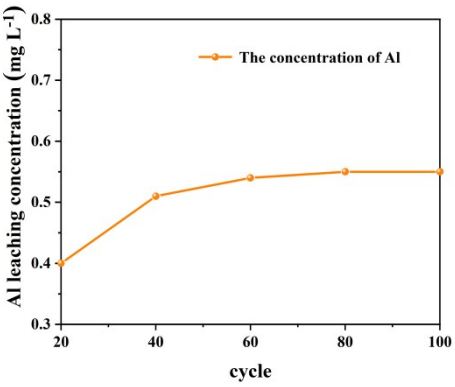

Fig. S7 The concentration of Al in the electrolyte during electrochemical base activation.

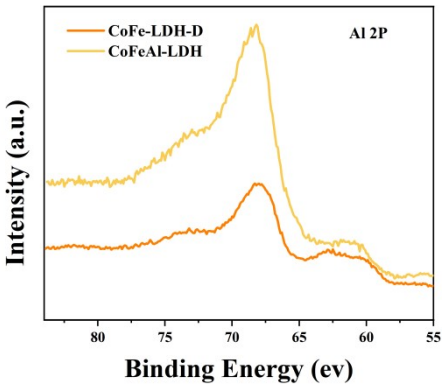

Fig. S8 Al 2P XPS of CoFeAl-LDH and CoFe-LDH-D.

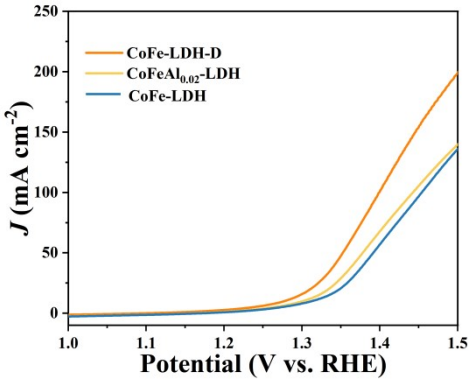

Fig. S9 The LSV of CoFe-LDH-D, CoFeAl-LDH and CoFe-LDH.

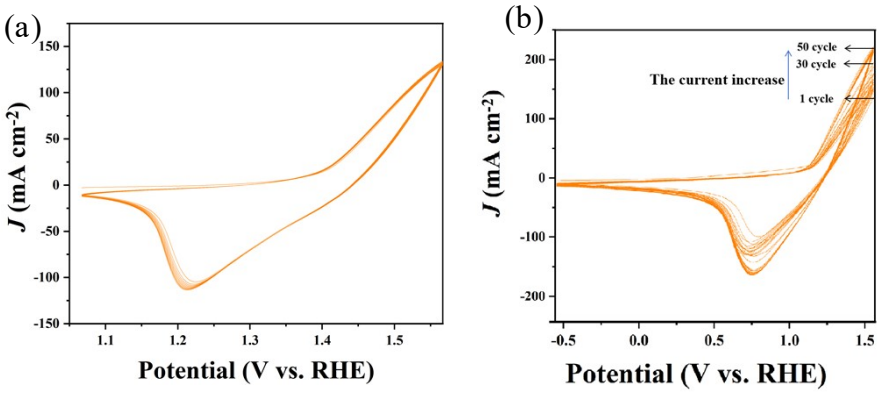

Fig. S10 The CV cycling curves of CoFeAl-LDH in the voltage range of 1.07 to 1.57 V *vs.* RHE and -0.57 to 1.57 V *vs.* RHE.

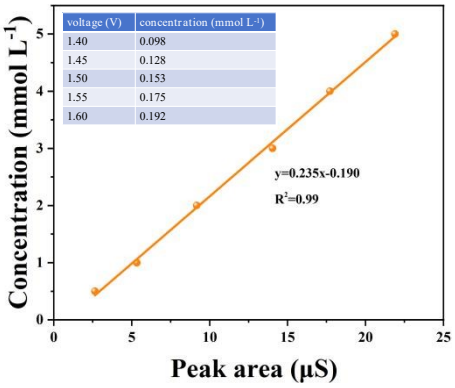

Fig. S11 The correction curve of the CH_3COO^-.

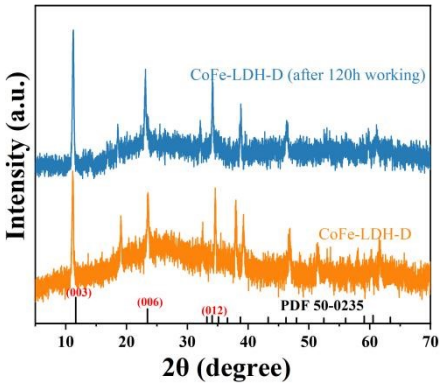

Fig. S12 XRD patterns of CoFe-LDH-D after working 120 h.

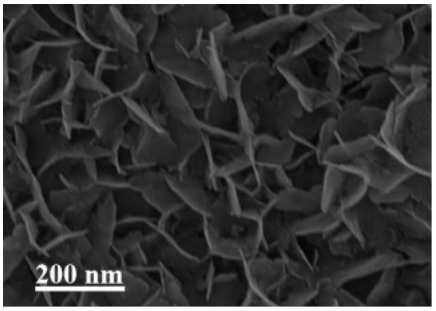

Fig. S13 SEM imagine of CoFe-LDH-D after working 120 h.

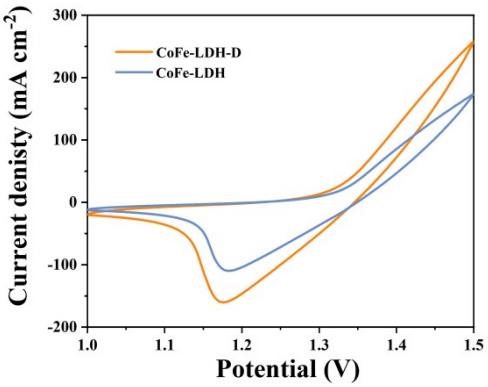

Fig. S14 The cyclic voltammetry (CV) curves of CoFe-LDH-D and CoFe-LDH in KOH-ethanol electrolyte.

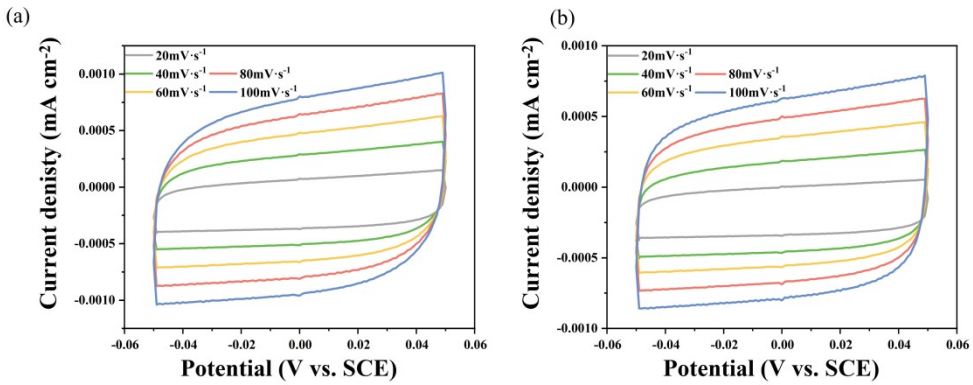

Fig. S15 The CV in the non Faradaic region of -0.05 to 0.05 V of (a) CoFe-LDH-D and (b) CoFe-LDH.

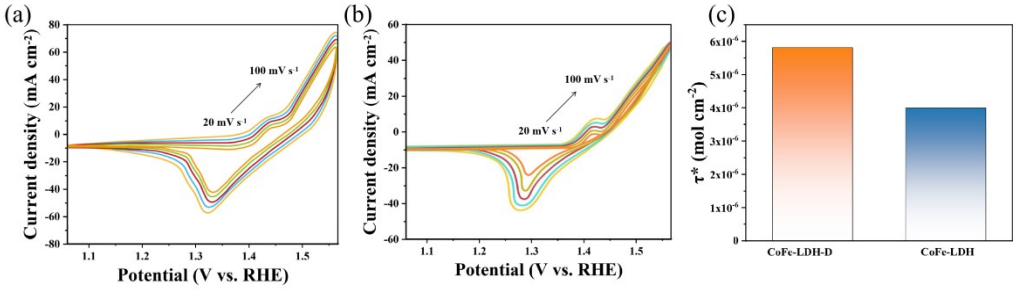

Fig. S16 CV curves of (a) CoFe-LDH-D and (b) CoFe-LDH in 1.0 M KOH in the potential range 1.07-1.57 V *vs.* RHE and at a scan rate of 20-100 mV s^{-1}.

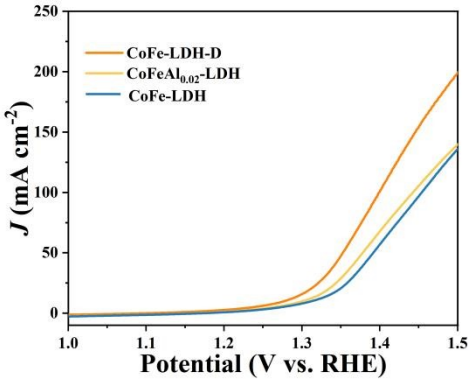

Fig. S17 LSV curves of CoFe-LDH-D, CoFeAl0.02-LDH and CoFe-LDH.

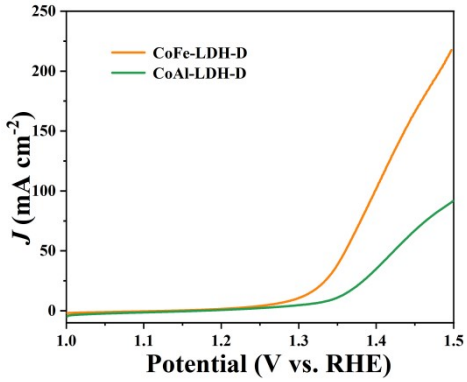

Fig. S18 LSV curves of CoFe-LDH-D and CoAl-LDH-D.

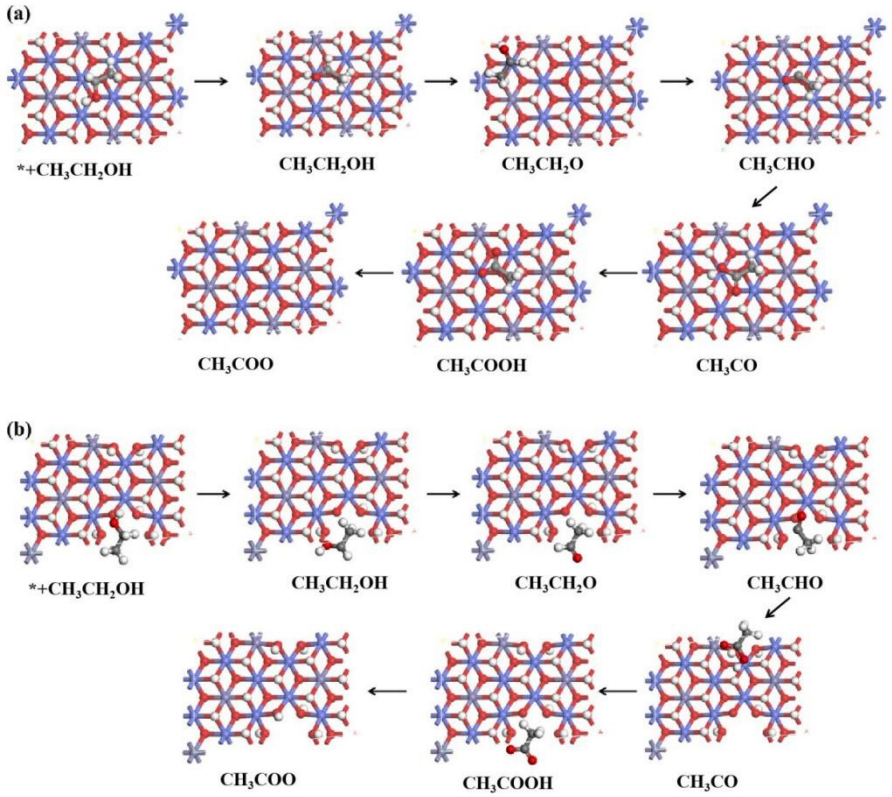

Fig. S19 The structure of CoFe-LDH and CoFe-LDH-D during the EOR process.

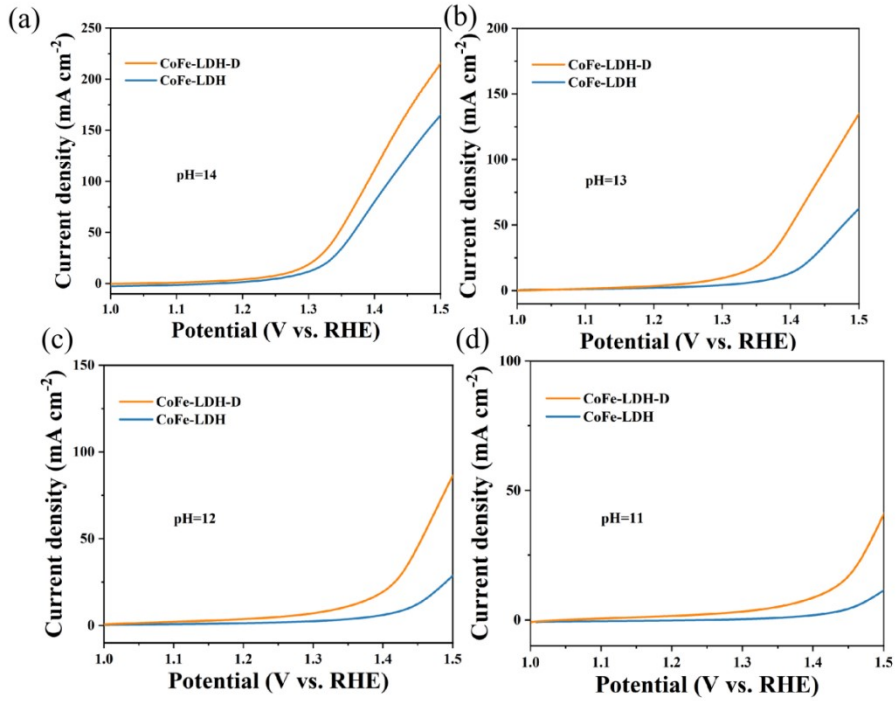

Fig. S20 The LSV of CoFe-LDH-D and CoFe-LDH at (a) pH=14, (b) pH=13, (c) pH=12, and (d) pH=11.